First Detection of 661 GHz ^{13}CO J=6→5: Large Amounts of Warm Molecular Gas

U.U. Graf[1], R. Genzel[1], A.I. Harris[1], R.E. Hills[2], A.P.G. Russell[1,3], and J. Stutzki[1,4]

[1] MPI für extraterrestrische Physik, Garching (FRG)
[2] MRAO, Cavendish Laboratory, Cambridge (UK)
[3] Joint Astronomy Centre, Hilo, Hawaii (USA)
[4] I. Physikalisches Institut, Universität zu Köln, Köln (FRG)

I. Introduction

Submillimeter and far-infrared observations of carbon monoxide (Jaffe, Harris, and Genzel 1987; Genzel, Poglitsch, and Stacey 1988; Schmid-Burgk et al. 1989; Boreiko, Betz, and Zmuidzinas 1989) have indicated the presence of warm, dense molecular gas near regions of recent star forming activity. Estimates based on the comparison of mid-J (submm) and high-J (far-IR) ^{12}CO lines in M17 and S106 (Harris et al. 1987a) gave a lower limit of $\approx 10^{18}$ cm^{-2} ($\tau(^{12}\mathrm{CO}\ 7\rightarrow 6) \approx 1$) to the CO column density of quiescent ($\Delta v \leq 10$ km/s) gas at temperatures of at least 100 K and H_2 densities of 10^4 to 10^6 cm^{-3}. The mid-J ^{12}CO lines are likely to be optically thick in most sources. In order to obtain a better estimate of the column densities, it is thus of great interest to observe isotopic mid-J CO lines, which are likely to be optically thin.

II. Observations and Results

The ^{13}CO J=6→5 (661.0673 GHz) detection was made on 1989 November 27 with the MPE cooled Schottky submillimeter heterodyne receiver (Harris et al. 1987b) mounted at the Nasmyth focus of the James Clerk Maxwell Telescope (JCMT), on Mauna Kea, Hawaii. On the same observing run we obtained complementary ^{12}CO J=6→5 and ^{13}CO J=3→2 data.

Strong ^{13}CO J=6→5 emission was detected from a number of positions toward Orion IRc2 (Fig. 1a)), Θ^1C, the Orion Bar, and NGC 2024 (Fig. 1b)). Both the ^{13}CO and the ^{12}CO J=6→5 spectra taken on Θ^1C and the Bar are affected by self-chopping due to the limited chop throw of 120″. These intensities are thus only lower limits.

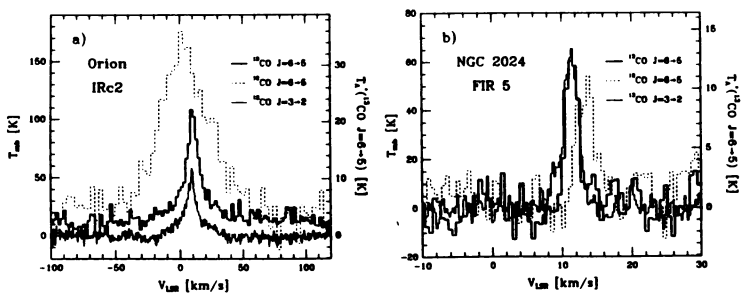

Fig. 1: CO lines detected toward Orion IRc2 (a)) and NGC 2024 (FIR 5, Mesger et al. 1988) (b)). The apparent velocity shift between the ^{13}CO lines and the main isotope in NGC 2024 is most likely caused by foreground absorption (Fig. 3).

III. Discussion

The ^{13}CO J=6 level lies 111 K above ground state. The J=6→5 transition has an A-coefficient of 1.9×10^{-5} s^{-1}, and in optically thin gas the critical density is $\approx 2\times10^5$ cm^{-3} (based

E. Falgarone et al. (eds.), Fragmentation of Molecular Clouds and Star Formation, 424–426.

on ^{12}CO collision rates given by Flower and Launay 1985). The high brightness temperature seen in this transition is an immediate proof of the presence of large amounts of warm, dense gas. In the optically thin limit a typical integrated line intensity of 120 K km/s (NGC 2024) implies a ^{13}CO column density in the J=6 level of 5×10^{15} cm^{-2}. Assuming LTE conditions, the maximum fractional population of the J=6 level is $\approx$11%. This constrains the total column density in warm ^{13}CO to $\geq5\times10^{16}$ cm^{-2}.

We compared the results from an escape probability, radiative transfer program (Stutzki and Winnewisser 1985) with the observed source parameters (Fig. 2). We base our radiative transfer analysis on the ^{13}CO lines only, since these are likely to have only moderate optical depths. The similarity of the ^{13}CO 6$\rightarrow$5 and 3$\rightarrow$2 line profiles supports the assumption that they arise from the same material. At 70 K $\leq T_{kin} \leq$ 400 K and densities $\geq10^5$ cm^{-3}, the ^{13}CO 6$\rightarrow$5/3$\rightarrow$2 ratio is a good measure of the kinetic gas temperature (Fig. 2). For the observed range of brightness temperatures the column density is constrained by the intensity of the ^{13}CO J=6$\rightarrow$5 emission to N(^{13}CO) = 4×10^{16}-5×10^{17} cm^{-2}. The 6$\rightarrow$5/3$\rightarrow$2 intensity ratio constrains the temperature to $\geq$100 K.

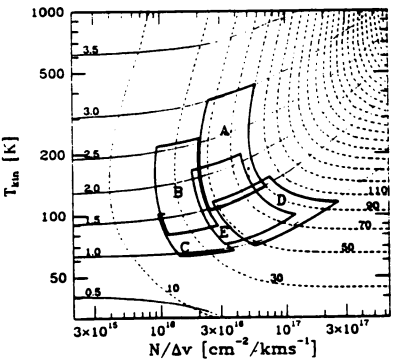

Fig. 2: Radiative transfer model of the ^{13}CO emission compared with the observed source parameters (Graf et al. 1990a). The model is calculated for an H_2-density of 10^6 cm^{-3}. We present the results in the two dimensional parameter space spanned by the kinetic gas temperature and the ^{13}CO column density per velocity interval. The dashed lines are curves of constant ^{13}CO J=6$\rightarrow$5 peak brightness temperatures, the dotted lines represent constant ratios of 6$\rightarrow$5/3$\rightarrow$2 peak brightness temperatures. The heavy boxes outline the range of parameters consistent with the observed values for the indidual sources: A: Orion IRc2 (spike), B: Orion IRc2 (plateau), C: Orion Bar (lower limits), D: NGC 2024 (0″,0″), E: NGC 2024 (-15″,15″).

IV. NGC 2024: Two Gas Components

The observations show an apparent velocity shift between the ^{12}CO and ^{13}CO J=6$\rightarrow$5 emission from NGC 2024. In addition, low-J, rare isotopic CO transitions (obtained with the IRAM 30m telescope with similar angular resolution) show rather complicated profiles (Fig. 3). the C^{17}O J=2$\rightarrow$1 profile is additionally affected by the presence of nuclear quadrupole hyperfine structure. We simultaneously fitted three lines (C^{17}O J=2$\rightarrow$1, C^{18}O J=2$\rightarrow$1 and ^{13}CO J=2$\rightarrow$1, Fig. 3) with two velocity components $T(v) = T_{ex} \times \{1 - \exp[-\tau \times \sum s_j \Phi(v - v_j)]\}$ along the line of sight. The foreground component can partially absorb the background component. The relative strength s_j of the different lines are given by the abundance ratios of the different isotopes (plus LTE excitation factors), or in the case of the C^{17}O hyperfine components by the spectroscopic factors.

A two velocity component model fits the data very well (Table 1). The fit identifies a cold foreground component with parameters very similar to the ones for the OH absorption component along the dust bar (Barnes et al. 1989). The warm background component agrees in velocity, velocity width and column density very well with the bulk emission from the molecular ridge (e. g. Moore et al. 1989 for CS observations). The column density is about twice that derived above for the warmer, ^{13}CO J=6$\rightarrow$5 emitting gas component. A temperature gradient in the warm component, with about 2/3 of the column density at temperatures around 50 K and 1/3 at temperatures around 200 K gives a consistent picture for all observed CO lines. In particular the apparent velocity shift between the ^{12}CO and ^{13}CO J=6$\rightarrow$5 lines can be explained by foreground absorption: with the excitation parameters of Table 1 the cold foreground component is optically thick ($\tau \approx 40$) in ^{12}CO J=6$\rightarrow$5 and has a low enough temperature to absorb essentially all of the ^{12}CO emission with velocities lower than $\approx$10 km/s. Due to the low temperature the opacity of the

https://doi.org/10.1017/S0074180900199243 Published online by Cambridge University Press

cold component drops rapidly with increasing rotational quantum number and indeed the observed ^{12}CO J=7→6 line (Graf et al. 1990b) is much brighter, slightly wider, and less "shifted" than the J=6→5 line.

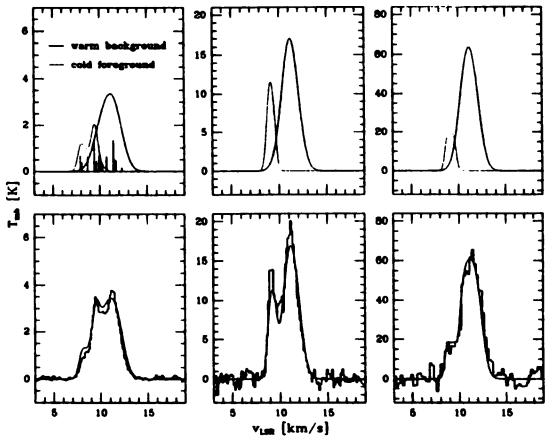

Fig. 3: Two component source model for NGC 2024 FIR 5, as derived from a simultanous fit to three low-J isotopic CO lines: $C^{17}O$ 2→1 (left; the upper panel shows the relative positions and intensities of the hyperfine components), $C^{18}O$ 2→1 (middle) and ^{13}CO 3→2 (right). The upper panels show the calculated emission from the two individual components: The two emission components add up to the line profiles shown in the lower panels, overlaid by the measured line profiles.

component	T_{ex} [K]	v_{LSR} [km/s]	Δv [km/s]	N_{H_2} [cm^{-2}]
foreground	18	9.2	0.8	4.0×10^{22}
background	70	11.2	2.0	2.2×10^{23}

Table 1: Fitted parameters of the two source components

V. What Heats the Gas?

The strong line emission detected in the ^{13}CO J=6→5 transition from both dynamically active and quiescent material confirms the presence of large amounts of warm, dense gas in star forming regions. Shocks, which are the dominant heating mechanism in the Orion plateau source (Draine and Roberge 1984, Chernoff, Hollenbach and McKee 1982), can be ruled out as a significant heating source in the other cases because of the narrow lines observed. Collisional heating of the gas by warm dust would require dust temperatures above 100 K which are highly unlikely because of the rapid increase of the dust cooling with temperature. Warm molecular gas is predicted to exist in photodissociation regions. However, all present models (e. g. Burton, Hollenbach, and Tielens 1990; Sternberg 1990), including recent extensions to higher densities, fail by about an order of magnitude to explain the observed ^{13}CO mid-J emission. See Graf et al. (1990a) for a more detailed discussion of the possible heating mechanisms.

References:

Barnes, P. J., et al. 1989, Ap. J., **342**, 883.

Boreiko, R. T., Betz, A. L., and Zmuidzinas, J. 1989, Ap. J., **337**, 332.

Burton, M., Hollenbach, D., and Tielens, A. G. G. M. 1989, 22nd ESLAB Symposium, "Infrared Spectroscopy in Astronomy"

Chernoff, D. F., Hollenbach, D. J., and McKee, C. F. 1982, Ap. J., **259**, L97.

Draine, B. T., and Roberge, W. G. 1984, Ap. J., **282**, 491.

Flower, D. R., and Launay, J. M. 1985, M.N.R.A.S., **214**, 271.

Genzel, R., Poglitsch, A., and Stacey, G. J. 1988, Ap. J., **333**, L59.

Graf, U. U. et al. 1990a, Ap. J. (Letters), in press.

Graf, U. U. et al. 1990b, in prep.

Harris, A. I., et al. 1987a, Ap. J., **322**, L49.

Harris, A. I., et al. 1987b, Internat. J. Infrared Millimeter Waves, Vol. 8, No. 8, p.857.

Jaffe, D. T., Harris, A. I., and Genzel, R. 1987, Ap. J., **316**, 231.

Mezger, P. G., et al. 1988, Astr. Ap., **191**, 44.

Moore, T. J. T., et al. 1989, M.N.R.A.S., **237**, 1p.

Schmid-Burgk, J., et al. 1989, Astr. Ap., **215**, 150.

Sternberg, A. 1990, in prep.

Stutzki, J., and Winnewisser, G. 1985, Astr. Ap., **148**, 254.

https://doi.org/10.1017/S0074180900199243 Published online by Cambridge University Press